International Journal of Modern Physics C
Vol. 24, No. 10 (2013) 1350065 (19 pages)

DOI: 10.1142/S0129183113500654

A MATHEMATICAL DESCRIPTION OF THE CRITICAL POINT IN PHASE TRANSITIONS

AYSE HUMEYRA BILGE* and ONDER PEKCAN†

Faculty of Engineering and Natural Sciences
Kadir Has University
Istanbul, Turkey
**ayse.bilge@khas.edu.tr*
†*pekcan@khas.edu.tr*

Received 30 January 2013
Accepted 31 May 2013
Published 6 August 2013

Let $y(x)$ be a smooth sigmoidal curve, $y^{(n)}$ be its nth derivative and $\{x_{m,i}\}$ and $\{x_{a,i}\}$, $i = 1, 2, \ldots$, be the set of points where respectively the derivatives of odd and even order reach their extreme values. We argue that if the sigmoidal curve $y(x)$ represents a phase transition, then the sequences $\{x_{m,i}\}$ and $\{x_{a,i}\}$ are both convergent and they have a common limit x_c that we characterize as the critical point of the phase transition. In this study, we examine the logistic growth curve and the Susceptible-Infected-Removed (SIR) epidemic model as typical examples of symmetrical and asymmetrical transition curves. Numerical computations indicate that the critical point of the logistic growth curve that is symmetrical about the point (x_0, y_0) is always the point (x_0, y_0) but the critical point of the asymmetrical SIR model depends on the system parameters. We use the description of the sol−gel phase transition of polyacrylamide-sodium alginate (SA) composite (with low SA concentrations) in terms of the SIR epidemic model, to compare the location of the critical point as described above with the "gel point" determined by independent experiments. We show that the critical point t_c is located in between the zero of the third derivative t_a and the inflection point t_m of the transition curve and as the strength of activation (measured by the parameter k/η of the SIR model) increases, the phase transition occurs earlier in time and the critical point, t_c, moves toward t_a.

Keywords: Gelation; phase transition; epidemic models.

PACS Nos.: 64.60.Bd.

1. Introduction

A phase transition is the passage of a physical system from one stable state to another. The abrupt passage from one state to the other is characterized by a "critical point" and a universal behavior near this critical point. Criticality in phase transitions have two aspects: The first aspect is criticality with respect to a system parameter p: Depending on the values of its structural parameters, a system may or may not undergo a phase transition spontaneously or under a driving force; there is a

critical value p_c such that for $p < p_c$ any perturbation of the system in the initial state dies out, while for $p > p_c$ the system evolves toward the final state, with the possibility of coexistence of both states in final equilibrium. The second aspect is the criticality with respect to time, characterized by a time t_c corresponding to the onset of the new phase. In most cases, provided that the system parameter p is larger than its critical value p_c the passage from one state to the other occurs abruptly in time, following a sigmoidal curve. The system also exhibits a universal behavior near the critical point, in the sense that the phase transition obeys a power law with possibly different exponents at the right and at the left of the critical point.

In the present paper, we shall propose a mathematical description of the critical point, as a point of fastest change, as given in Definition 2 of Sec. 3. The determination of the critical point defined above required the knowledge of the higher derivatives, at least, up to orders 20 to 30. The numerical precision of the standard methods we used was insufficient for this purpose, hence we had to use symbolic methods to compute higher derivatives. This required the availability of an exact solution which was practically possible only for test cases of standard mathematical functions and for the dynamical system representing the Susceptible-Infected-Removed (SIR) epidemic model. The SIR dynamical system was used recently as a mathematical model[1] for the gelation of polyacrylamide-sodium alginate (SA) composite (with low SA concentrations).[2] In this model the proportion of the "Removed" individuals was found to represent the sigmoidal gelation curve. We were able to solve the SIR model analytically as a dynamical system hence we could evaluate and plot higher derivatives with sufficient accuracy. Technical limitations of the present method and possible extensions to other gelation experiments are discussed in Sec. 5.2.

The general theory of the sol−gel transitions is given in Sec. 2.1. Gel formation is a typical phase transition in which monomers in a solution start forming polymer chains and when these disjoint chains combine to form an interconnected network, this is called a gel. Theoretical descriptions of the gelation has started in 1940's with the work of Flory and Stockmayer,[3,4] with the "mean field" or "classical" theory. An alternative description of the gelation is via the "percolation" scheme, as initiated in the work Stauffer[5] and used extensively later on.[6−8] In a simple percolation model, one considers a lattice with a given probability p for the sites being occupied. There is a critical probability of occupation p_c, below which the lattice is nonpercolating while above p_c it is percolating. Accordingly, if the probability of occupation increases in time, then there is a corresponding time t_c at which percolation starts. In the most general setting, if we consider the dynamical evolution of the site occupation on a lattice, the structural properties of the lattice or the propagation rules determine whether the time evolution of the system will lead to a phase transition or not. There is a drastic change in the final state at a critical value of the system parameter say p_c. For each parameter value $p > p_c$, for which the phase transition is guaranteed, there is a critical time t_c at which the phase transition occurs. In the case of polymerization and gel formation reactions, one should first of all prepare a setup that will lead to gel

formation, hence one works well in the region $p > p_c$ and the critical time at which gelation starts is called the "gel point" t_c.

Experimental monitoring of various gelation mechanisms has been published by Pekcan's group in a series of papers.[9–17] A review of these techniques, the determination of the critical point and the universal behavior near the critical point are reviewed in Sec. 2.2.

We present the motivation for the mathematical description of the critical point in Sec. 3. The idea is the following: The critical point is the junction of two curves, hence if we represent the phase transition by a single smooth curve, this property should be reflected in the behavior of the derivatives of the phase transition curve. The zero set of all derivatives[18] turns out to be an important tool to detect such behavior. In this section, we consider the logistic growth as a typical example of symmetrical sigmoidal curve and we illustrate the structure of the zero set of the derivatives and the convergence of their absolute extrema in Fig. 1.

SIR epidemic models[19] have been studied in the literature in the context of mathematical biology since as early as 1920's.[20] They were interpreted later on as percolation models, in which the spread of the epidemic throughout the society corresponds to percolation.[21] A variation of this model that takes into account the incubation period of the disease is the Susceptible-Exposed-Infected-Removed (SEIR) model. In a recent paper,[1] we have shown that the gelation of polyacrylamide SA with low SA concentrations obeying percolation results are represented by the SIR model while the curves for high SA concentrations agreeing with the classical results follow the SEIR model curves (Fig. 2). We describe these models in Sec. 4.1.

We present our main results in Sec. 4.2. In order to study the behavior of the critical point, we have computed higher derivatives of the SIR system analytically and plotted the normalized derivatives for a range of values of a key parameter in the SIR model. These results presented in Figs. 3–6(a) & (b) show that the critical point moves earlier in time as the strength of the activation increases. The location of these critical points agree qualitatively with the experiment, as presented in Sec. 5.1.

In Sec. 5.2, we discuss the limitations of our current numerical procedures and directions for future research.

2. The Sol–Gel Transition

2.1. *General theory*

Theoretical descriptions of the gelation has started in 1940's with the work of Flory and Stockmayer,[3,4] with the "mean field" or "classical" theory. These are statistical theories based on tree approximations where one assumes equal reactivities of functional groups and the absence of cyclization reactions. Most statistical theories derived in the following decades are fully equivalent, differing only in mathematical language,[22–25] e.g. the cascade theory by Gordon.[22] The "site percolation model" is based on a lattice where the sites are either empty or filled. In the representation of the sol−gel transition, empty sites represent monomers and filled sites represent

bonded monomers that form a polymer chain; the gel state corresponds to the onset of percolation. Alternatively, one can consider the "bond percolation model" in which the monomers occupy the nodes of the lattice and the bonds among monomers are represented by the edges joining these nodes. Both the classical theory and the percolation theories predict that monomers start to agglomerate in the sol phase until a point where gel formation starts and the gel phase dominates. Both theories exhibit a universal behavior near the gel point in the sense that various quantities describing the phenomena are of the form of a power function $|t - t_c|^{\alpha}$ for a variety of experimental conditions. The critical exponents for the "weight average degree of polymerization, S" before the critical point and the "gel fraction G" after the critical point, denoted respectively by γ and β are of prime importance. In experimental setups, the fluorescence intensity measures these exponents at both sides of the critical point.[9] The difference between the Flory−Stockmayer and the percolation theories is reflected to the values of the critical exponents.

2.2. *Experimental techniques*

In this section, we describe experimental techniques for monitoring the gelation mechanism in various systems. The application of the present method to these situations is discussed in Sec. 5.2.

(a) *The gelation of poly(methyl methacrylate) (PMMA) with the fast transient fluorescence (FTRF) technique*[10]: The FTRF technique was used to study the critical exponents during glass transition in free-radical cross-linking copolymerization (FCC). Pyrene (Py) was used as a fluorescence probe and its fluorescence lifetimes from its decay traces were measured during glass transition. Changes in the viscosity of the pre-gel solutions due to glass formation dramatically increased the Py fluorescent lifetimes, which were used to study the glass transition as a function of time. The results were interpreted in the view of percolation theory. The critical exponents, β and γ, were found to be around 0.37 ± 0.015 and 1.69 ± 0.05, respectively. In fitting the data, a main obstacle lies in the precise determination of the glass point and the critical region. The way to find the critical point in real experiments is to measure and to perform the scaling analysis for more than one quantity. The critical point can then be determined by varying p_c in such a way as to obtain good scaling behavior for both quantities over the greatest range in $|p - p_c|$, or $|t - t_c|$ if the experiments are performed against time.

(b) *The gelation of poly(methyl methacrylate) (PMMA) with steady-state fluorescence (SSF)*[9]: In this experiment, gelation was monitored by fluorescence intensity and it has been found that the sigmoidal curves obey the percolation model. The critical exponents were measured at both sides of the critical point, as described in the previous experiment. The critical point, located by scaling, was found to be relatively close to the inflection point of the sigmoidal curve.

(c) *The gelation of acrylic materials with photo-differential scanning calorimetric (Photo-DSC)* technique[11]: A (Photo-DSC) technique was used to study the photo-initiated radical polymerization. It was observed that all conversion curves during gelation at various UV light intensities present good sigmoidal behavior as predicted by the percolation model. Observations around the critical time, called the glass transition point (t_g), taken for polymerization to reach the maximum rate (R_{pmax}) showed that the gel fraction exponents β obeyed the universal percolation picture. The values of the β exponents were determined from the slope of the straight lines from the double logarithmic plot of the conversion versus time curves above t_g. The time corresponding to the maximum of the rate of polymerization was chosen as the critical time, t_c, which may be named as the glass transition point, t_g, for the photo-initiated gelation under consideration. In this experiment the observed gelation curve corresponded to the post-critical part of the sigmoidal curve and consequently only the exponent β has been found.

(d) *The gelation of acrylamide (AAm) with SSF*[12]: The sol–gel transition for the free radical cross-linking polymerization of AAm was studied using the SSF technique. In this study, Pyranine was used as a fluoroprobe for monitoring the polymerization. The fluorescence intensity of the Pyranine bonded to the gel, versus reaction time, was used to recover the critical exponents β and γ. The gel fraction exponent β and the weight average degree of polymerization exponent γ agree best with the static percolation results for higher AAm concentrations above 1 M, but they cross over from percolation to mean-field Flory–Stockmayer values when the AAm concentration is lower than 2 M. For determining the gel points, each experiment was repeated at the same experimental conditions, and the gel points were obtained by a dilatometric technique. A steel sphere of 4.8 mm diameter was moved in the sample up and down slowly by means of a magnet applied to the outer face of the sample cell. The time t_c at which the motion of the sphere was stopped was evaluated as the onset of the gelation.

(e) *The gelation of AAm with SA via SSF*[2]: In this experiment, the gelation of polyacrylamide (AAm) SA was monitored by SSF technique. A crossover from percolation to classical model was observed as in (d) above as the SA concentrations were increased. The gelation curves of these experiments with low SA concentrations obeying percolation results are represented by the SIR model while the curves for high SA concentrations agreeing with the classical results follow the SEIR model curves.[1]

(f) *The gelation of bio-gels with photon transmission technique*[13–15]: In these experiments, the gelation of Carrageenan was monitored with a photon transmission technique. These experiments are characterized by the reversibility of the gelation with temperature and by the hysteresis between the cooling and heating curves. In these experiments, only the post critical point exponent β was measured.

(g) *The gelation of poly(methyl metacrylate) (PAAm) and bio-gel composites with SSF technique*[16]: In this experiment, the gelation of PAAm and Carrageenan

composite was monitored with SSF technique. The experiment was characterized by a crossover from percolation to classical results, where only the post critical point exponent β was measured.

(h) *The gelation of poly(methyl metacrylate)* (*PAAm*) and carbon nanotube composites with SSF technique[17]: In this experiment, the gelation of PAAm doped with carbon nanotubes has been monitored both with fluorescence and resistivity measurements. The fluorescence intensity yielded only the post critical point exponent β. This experiment was characterized by a percolation model. Here, the critical exponent for the conductivity was also recovered and found to be around 2.0.

All these experiments provide us various sigmoidal curves obeying either percolation or classical models near a critical point. The present paper is based on the results of the experiment (e), the gelation of the AAM-SA, with low SA concentrations. Possible tests our mathematical model to locate the critical points of other physical and/or chemical system using their sigmoidal curves are discussed in Sec. 5.2.

3. Mathematical Description of the Gel Point

In the present paper, we will give a mathematical characterization of critical points as the common limit of the sequence of points where the even and odd derivatives of the phase transition curve reach their absolute extremum.

The phase transition can be modeled by a function $y(x)$ that represents a measurable property of the system, where x is either time or a system parameter. The critical value of x at which the phase transition occurs is called the "critical point" and it is denoted by x_c. We shall also use the term "phase transition point" or the "gel point," to emphasize its nature.

The physical laws governing the system at the initial phase where $x < x_c$ and at the final phase where $x > x_c$ may be different. Hence, one may expect that the phase transition curve $y(x)$ has different functional forms before and after critical point. Furthermore, it is also conceivable that the laws that govern the initial phase still give rise to measurable effects after the critical point. We may also assume that the function that represents the evolution of the initial phase before and after the critical point is continuous at x_c and symmetric about $x = x_c$. These considerations lead to the generally accepted functional form

$$y(x) = \begin{cases} f(|x - x_c|), & x < x_c; \\ y_c, & x = x_c; \\ Kf(x - x_c) + h(x - x_c), & x > x_c, \end{cases} \tag{1}$$

where K is a constant, f and h are smooth functions with horizontal asymptotes as x goes to infinity. Junction conditions ensure that $y(x)$ is continuous at x_c, but

there is no guarantee that it will be differentiable and its higher derivatives will exist at this point. Nevertheless, if the system is described by a dynamical system $y' = F(y)$ where F is smooth, as what usually is done, the solutions will also be smooth curves. One would then expect the nonanalyticity at the junction point to be reflected in the behavior of the derivatives around the critical point. This will be our point of view in "defining" the point where the phase transition occurs, as a point where the derivatives of the transition curve display a "strange" behavior. Our approach will be to model a phase transition by a dynamical system, study the behavior of its higher derivatives and give a definition of the critical point based on mathematical properties of the sigmoidal curve representing the transition. This will be illustrated on the solutions of the SIR dynamical system as a model for sol−gel transition.

Let $y(x)$ be a smooth, monotone function that represents a phase transition. Since the initial and final states are stable, the function $y(x)$ should have distinct horizontal asymptotes, that might be scaled to 0 and 1, as x goes to $\pm\infty$ and its higher derivatives should vanish in these limits. A basic property of continuous functions is that if they vanish at two points x_1 and x_2, they have a horizontal tangent at some point in between. Thus, the first derivative $y'(x)$ has at least one point with a horizontal tangent and the second derivative $y''(x)$ has at least one zero. By similar arguments one can conclude that the nth derivative $y^{(n)}$ has at least $n-1$ zeros. A sigmoidal curve y where $y^{(n)}$ has exactly $n-1$ zeros is, in a sense, a curve which makes no "unnecessary oscillations". We will call such a curve a "basic sigmoidal curve".

Definition 1. A *basic sigmoidal curve* is a curve $y(x)$ such that

$$\lim_{x\to-\infty} = 0, \quad \lim_{x\to\infty} = 1, \quad \lim_{x\to\pm\infty} y^{(n)}(x) = 0, \quad \text{for all } n$$

and $y^{(n)}(x)$ has exactly $n-1$ zeros.

The set of points where the nth derivative $y^{(n)}$ reaches its extreme values corresponds to the set of zeros of $y^{(n+1)}$. We can thus study the properties of the zero set of all derivatives of a function in order to investigate the growth behavior of its derivatives. The condition of Definition 1 induces some regularity to the sequence of zeros of the derivatives, namely the zeros of successive derivatives alternate. Note that, local extrema of $y^{(n)}$ correspond to the zeros of $y^{(n+1)}$ and its inflection points to the zeros of $y^{(n+2)}$. We can illustrate the ordering of the zeros, starting by the inflection point of $y(x)$. If we denote the ith zero of $y^{(n)}$ by x_n^i, the inflection point of $y(x)$ is the unique zero of its second derivative $y^{(2)}$, denoted by x_2^1. Clearly x_2^1 lies in between the two zeros of the third derivative x_3^1 and x_3^2, and we have the order relations $x_3^1 < x_2^1 < x_3^2$. The fourth derivative has three zeros, satisfying the order relations

$$x_4^1 < x_3^1 < x_4^2, \quad x_4^2 < x_3^2 < x_4^3.$$

Here, we see that although the zeros of the third and fourth derivatives alternate, we cannot say anything about the relative positions of x_2^1 and x_4^2. Thus, the observed regular behavior of the zeros near the "critical point" to be defined below is not a straightforward consequence of the alternation of zeros of successive derivatives.

The properties of the zeros of the derivatives of a function $y(x)$ were addressed in an expository talk in 1942 by Polya[18] who posed a number of problems on the behavior of the sets of zeros of the derivatives. He defined the notion of the "final set" which is the set of points p such that every neighborhood of p contains a zero of an infinite number of derivatives. For example if $y = \sin(x)$, the points $x = k\frac{\pi}{2}$ belong to the final set. If $y(x)$ is an odd sigmoidal function, then all derivatives of y vanish at $x = 0$ and this point belongs to the final set. Polya's review talk deals first with complex functions and discusses the structure of the final set first for functions with singularities then for entire functions that are regular everywhere. For entire functions, the final set depends on the "order" of the function, which is related to its rate of growth at infinity; for functions of order greater than 1, differentiation tends to make the final set denser, while if the order is less than 1 the final set becomes thinner; precise formulations being given in Ref. 18. There are a number of claims on the relation of the order of a function and the structure of the final set. In particular, Polya conjectures that "if a real entire function of order greater than 1 remains bounded for real values of the independent variable, then its final set contains the whole real axis". Subsequent work on the questions posed by Polya, deal with the relation of the set of zeros to the analyticity properties of the function, we can cite Refs. 26 and 27 among a few. The result that is relevant in our work is the fact that the final set of a meromorphic function is the boundary of the domains of the poles. We recall that a meromorphic function is analytic except for poles and we note that the analytic continuation of a sigmoidal function is necessarily meromorphic. The domain of a pole a is the set of points whose distances to the pole a are smaller than their distances to any other pole. Since complex poles should occur in conjugate pairs, the real axis is a boundary of the domains of a pair of conjugate poles. It follows that all points of the real line belong to the final set in particular there should be no gap in the set of zeros of the derivatives.

We will describe the critical point of a phase transition by the concurrence of the absolute extreme values for the derivatives. Clearly the extrema of odd derivative correspond to the zeros of even derivatives and vice versa. Thus, if the critical point is to represent some type of break-point, the best that we can expect is that the sequences, $\{x_{m,i}\}$ and $\{x_{a,i}\}$, formed by the points where the even and odd derivatives reach their extreme values respectively, converge to a common limit point x_c. Note that the fact that the whole real line consists of the final set does not guarantee the convergence of these sequences. Furthermore, even if they converge, there is *a priori* no reason for the equality of their limits. In fact, in our preliminary computations, we have seen that the convergence rates of the sequences $\{x_{m,i}\}$ and $\{x_{a,i}\}$ are different and there seems to be a gap in the set of zeros as seen in Figs. 13–6(a).

In the case of the logistic growth, we were able to compute derivatives up to order 200, hence "see" that both of the sequences above have the same limit. The computation of the derivatives up to such high orders was not possible for the SIR model. The notion of the final set is thus crucial in concluding that there should be no gaps in the set of zeros. Based on these considerations, we propose the following definition for the "critical point".

Definition 2. Let $y(x)$ be a basic sigmoidal curve and let $\{x_{m,i}\}$ and $\{x_{a,i}\}$ be the sequence of points where the even and odd derivatives $y^{(2i)}$ and $y^{(2i+1)}$ reach their absolute extremum. If these sequences converge and they have the same limit x_c, then x_c is called the "critical point of the sigmoidal curve."

We note that, if time is re-scaled, the magnitude of the derivatives also are re-scaled and it is possible to arrange this scaling such that all derivatives of a sigmoidal curve decay as the order of differentiation decreases. From this we conclude that the unbounded growth of the derivatives near a point is not an invariant property but the structure of the normalized derivatives and their zero set is more meaningful as an indicator of the threshold of a phase transition represented by a sigmoidal curve.

Note that since a sigmoidal curve is monotone, one can as well parametrize the higher derivatives in terms of y and work in a compact domain. For example, the standard logistic growth curve is characterized by the first-order ordinary differential equation

$$\frac{dy}{dt} = 1 - y^2.$$

Higher derivatives of y with respect to time, denoted by $\frac{d^n y}{dt^n} = y^{(n)}$ can be computed recursively using the chain rule, by the formula

$$y^{(n)} = \frac{dy^{(n-1)}}{dy}\frac{dy}{dt} = \frac{dy^{(n-1)}}{dy}(1 - y^2).$$

The plot of the normalized derivatives up to order 30 for the logistic growth is given in Fig. 1(a). It can be seen that $y = 0$ is a concurrent extremum of odd derivatives, hence a common zero of the even derivatives. There seems to be a gap surrounding $y = 0$ in the zero set, but in fact, the zeros of the odd derivatives are symmetrical about $y = 0$ and the converge to $y = 0$, but the convergence is very slow. The convergence of the first zero of odd order derivatives is displayed in Fig. 1(b). Computationally it was possible to compute the derivatives up to order 200 analytically and find the root nearest to $y = 0$ numerically but it was possible to plot these derivatives simultaneously only up to order 30.

The same structure has been observed for a number of symmetrical sigmoidal curves and we may expect that this behavior can be representative of the symmetrical phase transitions. The asymmetric case seems to be more interesting, as illustrated by the behavior of the SIR model solutions.

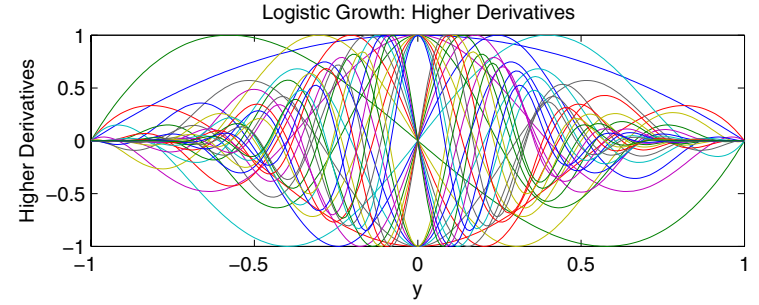

(a)

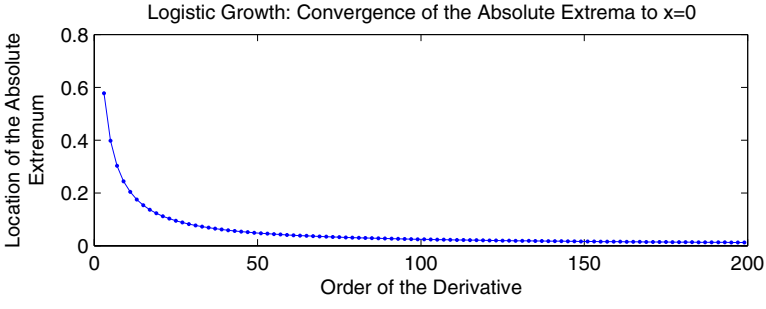

(b)

Fig. 1. (Color online) (a) The first 30 normalized derivatives of the logistic growth curve satisfying the differential equation $dy/dt = (1 - y^2)$, plotted with respect to y. The point $y = 0$ is the common zero of all even derivatives and in fact the absolute extremum for all odd derivatives. The absolute extrema of the even derivatives is symmetrical about $y = 0$. The point $y = 0$ seems to be isolated, but the zeros of odd derivatives approach $y = 0$ as the order of differentiation increases. (b) The location of the zero of the odd derivatives that is closest to $y = 0$. The sequence converges to $y = 0$, but quite slowly.

4. The SIR Model

In a previous paper,[1] we have modeled the sol−gel transition curves observed experimentally as reported in Ref. 2, by a dynamical system representing the spread of epidemics in a closed society.[19] Motivated by the idea that the gel point should be a point where there should be something "wrong" with derivatives, we have computed higher derivatives of the SIR system up to orders 20 to 30. Surprisingly, a plot of the normalized derivatives displayed a "strange behavior" at a point in between the zeros of the third and second derivatives of the phase transition curve, where the gel point is expected to be located. We have then repeated the computations for various parameter values and we have shown that the proposed candidate for the gel point moves back from right to left in time, i.e. from the inflection point to the zero of the third derivative, as the steepness of the transition curve increases. We report and discuss these simulation results in the present work. We first present the SIR model in Sec. 4.1 then we illustrate the determination of the critical point as given in Definition 2 in Sec. 4.2.

4.1. *The SIR dynamical system*

The differential equations governing the SIR epidemic model are

$$\frac{dS}{dt} = -kSI, \quad \frac{dI}{dt} = kSI - kI, \quad \frac{dR}{dt} = \eta I.$$

The rate of change in the sum $S + I + R$ is zero, hence by normalizing the total population, we can set $S + I + R = 1$. A variation of the SIR model is the SEIR model that involves an incubation period (the "Exposed" individuals) during which the individual cannot communicate the disease to other people. The differential equations governing this system are

$$\frac{dS}{dt} = -kSI, \quad \frac{dE}{dt} = kSI - \epsilon E, \quad \frac{dI}{dt} = \epsilon E - \eta I, \quad \frac{dR}{dt} = \eta I.$$

Here also the total population is normalized as $S + E + I + R = 1$. These dynamical systems have been used in a previous paper,[1] to model the gel formation of polyacrylamide with SA with different concentrations of SA. We have shown that low activation experiments (with high SA concentrations) obey the SEIR model while the high activation models (with low SA concentrations) obey the SIR model. The experimental observations, and their measured gel points are shown in Fig. 2.

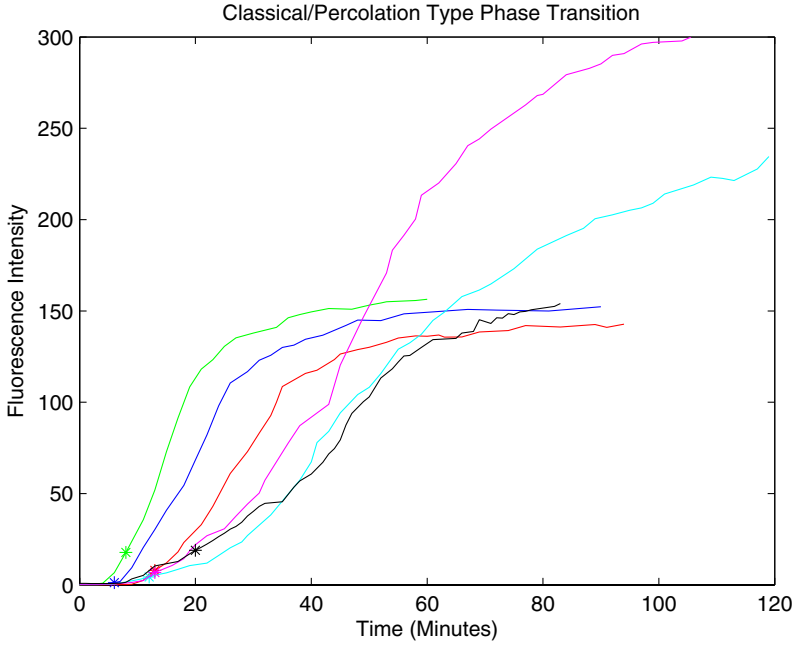

Fig. 2. (Color online) The experimental gelation curves for polyacrylamide-SA. The steep, low amplitude curves correspond to low SA concentrations obeying percolation model while the slower rising high amplitude curves obey classical model. The gel points are determined by a dilatometric technique.

The determination of the phase transition point of a function $y(x)$ as proposed in Definition 2, requires the computation of the derivatives up to orders 20 to 30 and plotting their graph simultaneously. In practice, this requires either the availability of exact solutions or very precise numerical procedures. We have obtained an exact solution for the SIR dynamical system, then used the symbolic programming language REDUCE to compute higher derivatives.

In the case of the SIR model, I is solved explicitly in terms of S by integrating $\frac{dI}{dS} = \frac{dI}{dt} / \frac{dI}{dS}$ with the initial conditions $S(0) = S_0$, $I(0) = 1 - S_0$. We then have an exact expression for I as a function of S.

$$I = 1 - S + \frac{\eta}{k} \ln(S/S_0).$$

We will use the expression above to compute higher derivatives of R with respect to t as follows. Since $S(t)$ is a monotone function of time, it can be used as parameter and the chain rule relates the derivatives with respect to t and S of a function $f(t)$ as $\frac{df}{dt} = \frac{df}{dS}\frac{dS}{dt} = -kSI\frac{df}{dS}$. Then, since $dR/dt = \eta I$ is known as a function of S, the second derivative with respect to time, $\frac{d^2R}{dt^2} = -k\eta SI\frac{dI}{dS}$, is also expressed as a function of S. One can then evaluate higher derivatives with respect time iteratively. This has been done with the symbolic programming REDUCE, and within the limitations of the present computational tools, we were able to compute the first 30 derivatives analytically. As the expression of the derivatives of R directly as a function of t requires numerical computations and displays instabilities at high orders we have preferred to plot the derivatives of R as a function of S. Similarly, as there is no exact solution for the SEIR system even as a function of S, we had to use numerical solutions of the SEIR system. The results were unsatisfactory within our present computational methods and we decided to restrict our presentation to the SIR model.

4.2. *The critical point for the SIR model*

We have studied the behavior of the zeros of the function $R(t)$ for different values of the parameter k/η, by choosing $S_0 = 0.9$, $\eta = 1$ and $k = 2, 3, 4, 5, 10, 20$. We have summarized these results in Table 1, but we have presented the graphs for $k = 3, 4, 5, 10$ only in Figs. 3–6(a) & (b). The derivatives were normalized to 1 and plotted simultaneously as presented in Figs. 3(a)–6(a). As noted in the previous subsection, the normalized derivatives can be viewed as functions of t or S; they are graphed as a function of S, instead of t, for avoiding numerical instabilities. From Figs. 3(a)–6(a), it can be seen that there is a point S_c, indicated by $(*)$ on the horizontal axis, nearby which, a large number of normalized derivatives reach the values 1 or -1. Since the $(n+1)$th derivative should vanish at the maxima and the minima of the (n)th derivative, a large number of curves cross zero near that same point. Here, near S_c, derivatives of even order reach their absolute extreme values while derivatives of odd order are zero. The point S_c falls between the maximum and the inflection point of I. The sequence of points where the derivatives

Table 1. The locations of the maximum of I (S_m and t_m), the inflection point of I (S_a and ta) and the critical point (S_c and t_c) in terms of S and t for various values of the SIR model parameter k/η.

k/η	S_m	S_c	S_a	t_m	t_c	t_a
2	0.500	0.722	0.828	1.772	0.363	0.821
3	0.333	0.632	0.718	1.383	0.501	0.687
4	0.250	0.594	0.665	1.097	0.437	0.538
5	0.200	0.573	0.633	0.910	0.373	0.436
10	0.100	0.534	0.568	0.503	0.205	0.221
20	0.050	0.517	0.535	0.277	0.106	0.110

reach the maxima of their absolute values were computed numerically and it has been observed that the subsequence given by even order derivatives approaches to a value S_c quite fast. The time domain plots of S, R and I are given in Figs. 3(b)–6(b). In these figures, we have indicated the inflection point of $R(t)$, t_m by $(*)$. The zero of

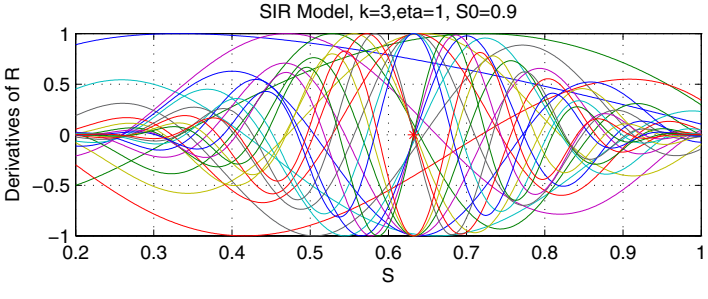

(a)

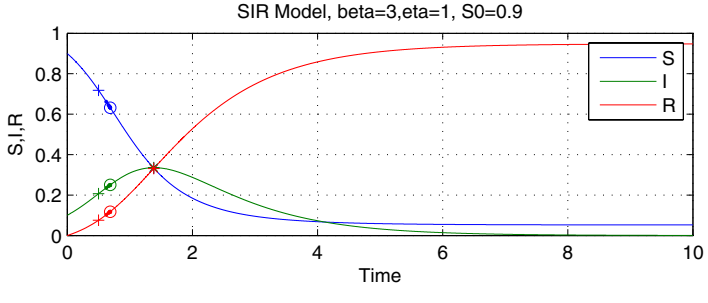

(b)

Fig. 3. (Color online) (a) The first 24 derivatives of $R(t)$ normalized to 1 for $k = 3$, $\eta = 1$ and $S_0 = 0.9$. The curves are plotted against $S(t)$. The phase transition point, indicated by $(*)$ is expected to be located at $S_c = 0.632$. (b) The time domain plots of the solution curves S, I, R. $S(t)$ is monotone decreasing while $R(t)$ is monotone increasing. The sequence of points converging to the phase transition point t_c are shown on each curve by $(.)$. The phase transition point t_c indicated by (o), is located between the maximum of zero I, t_m denoted by $(*)$ and the inflection point of I, t_a denoted by $(+)$. For $k = 3$, t_c is located at 78% left of t_m in the interval (t_a, t_m).

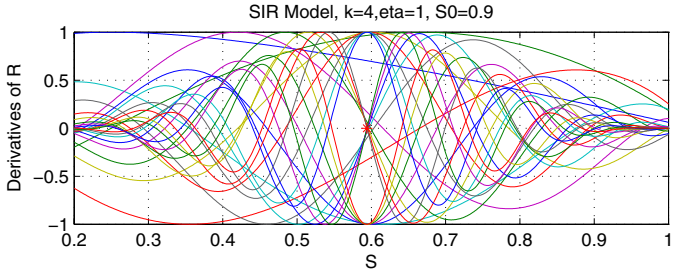

(a)

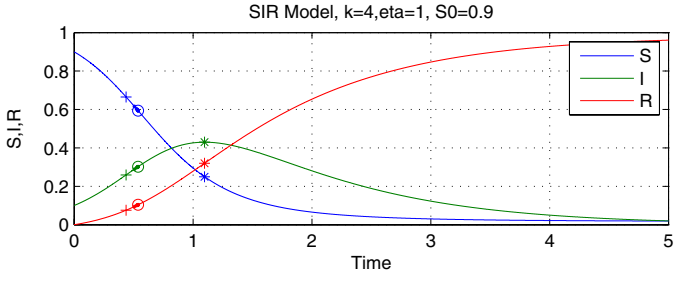

(b)

Fig. 4. (Color online) (a) The first 24 derivatives of $R(t)$ normalized to 1 for $k = 4$, $\eta = 1$ and $S_0 = 0.9$. The curves are plotted against $S(t)$. The phase transition point, indicated by $(*)$ is expected to be located at $S_c = 0.594$. (b) The time domain plots of the solution curves S, I, R. $S(t)$ is monotone decreasing while $R(t)$ is monotone increasing. The sequence of points converging to the phase transition point t_c are shown on each curve by $(.)$. The phase transition point t_c indicated by (o), is located between the maximum of zero I, t_m denoted by $(*)$ and the inflection point of I, t_a denoted by $(+)$. For $k = 4$, t_c is located at 84% left of t_m in the interval (t_a, t_m).

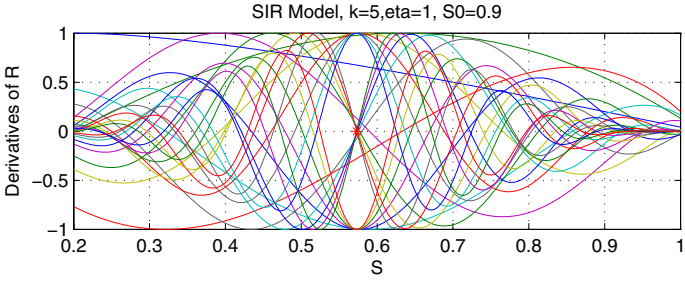

(a)

Fig. 5. (Color online) (a) The first 24 derivatives of $R(t)$ normalized to 1 for $k = 5$, $\eta = 1$ and $S_0 = 0.9$. The curves are plotted against $S(t)$. The phase transition point, indicated by $(*)$, is expected to be located at $S_c = 0.573$. (b) The time domain plots of the solution curves S, I, R. $S(t)$ is monotone decreasing while $R(t)$ is monotone increasing. The sequence of points converging to the phase transition point t_c are shown on each curve by $(.)$. The phase transition point t_c indicated by (o), is located between the maximum of zero I, t_m denoted by $(*)$ and the inflection point of I, t_a denoted by $(+)$. For $k = 5$, t_c is located at 88% left of t_m in the interval (t_a, t_m).

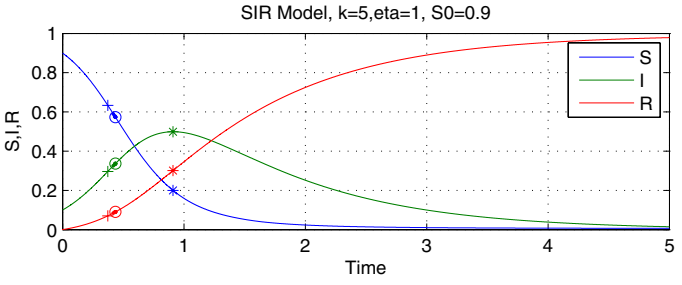

(b)

Fig. 5. (*Continued*)

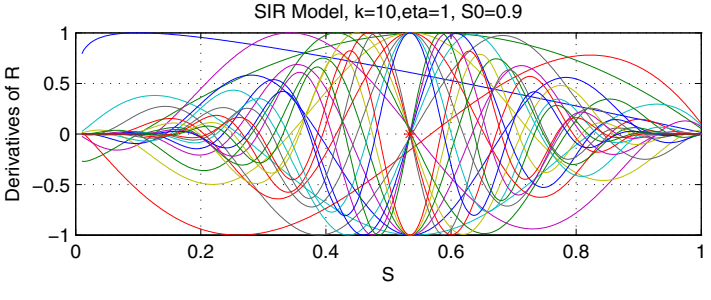

(a)

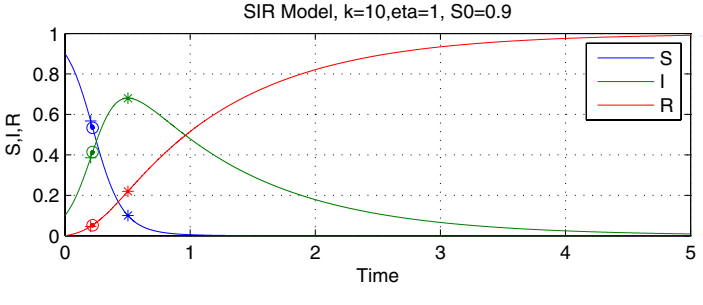

(b)

Fig. 6. (Color online) (a) The first 24 derivatives of $R(t)$ normalized to 1 for $k = 10$, $\eta = 1$ and $S_0 = 0.9$. The curves are plotted against $S(t)$. The phase transition point, indicated by $(*)$, is expected to be located at $S_c = 0.534$. (b) The time domain plots of the solution curves S, I, R. $S(t)$ is monotone decreasing while $R(t)$ is monotone increasing. The sequence of points converging to the phase transition point t_c are shown on each curve by $(\cdot)$. The phase transition point t_c indicated by (o), is located between the maximum of zero I, t_m denoted by $(*)$ and the inflection point of I, t_a denoted by $(+)$. For $k = 10$, t_c is located at 94% left of t_m in the interval (t_a, t_m).

the third derivative, i.e. the inflection point of I, that we have denoted by t_a is indicated by $(+)$. The sequence of the extrema of the even order derivatives are shown by $(.)$ in these figures. The limiting value of this subsequence is the proposed gel point t_c, shown with (o). These values are listed in Table 1, where (S_m, S_c, S_a) and (t_m, t_c, t_a) denote respectively the maximum of I, the phase transition point and the inflection point of I. From these figures, we see that for the SIR model, for low values of the parameter k/η, the proposed phase transition point is closer to the maximum of I while for higher values of k/η it moves toward the inflection point of I.

The location of the gel point with respect to the zero of the third and second derivatives is shown in Figs. 7(a)−7(d), for $k = 3, 4, 5, 10$ and $\eta = 1$. In these figures, we have given a plot of $R(t)$, as the model of the gelation curve, with respect to t, for

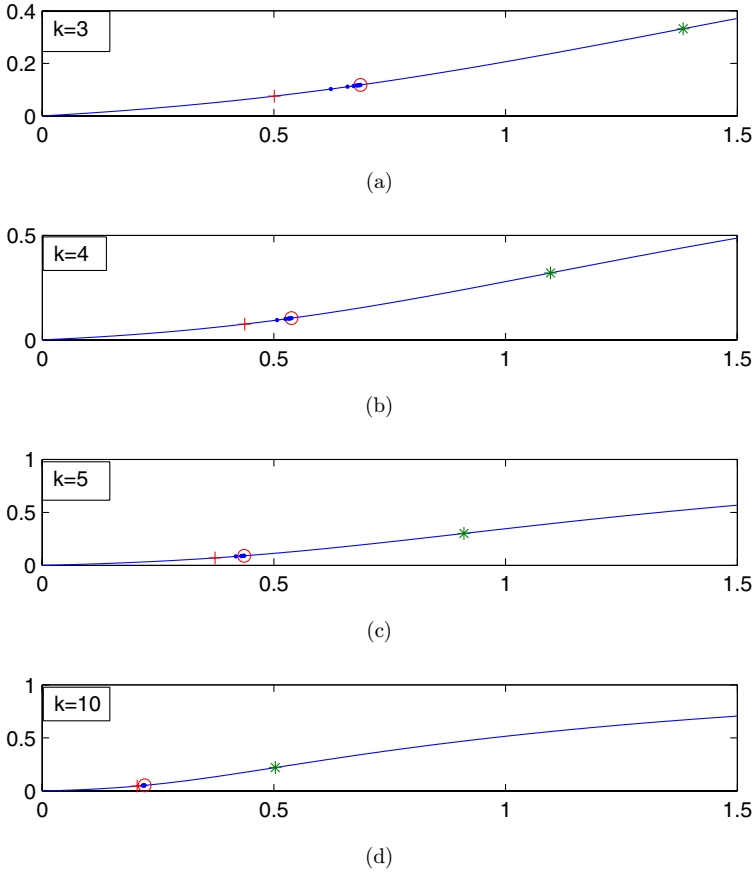

Fig. 7. (Color online) (a)−(d) The location of the gel point with respect to the zero of the third and second derivatives, for $k = 3, 4, 5, 10$ and $\eta = 1$. $R(t)$, as the model of the gelation curve is plotted with respect to t, for the initial portion of the gelation. The zero of the second derivative, i.e. the inflection point of the gelation curve is shown by $(*)$, while the zero of the third derivative is denoted by $(+)$. The sequence of the absolute maxima of the even order derivatives are shown by $(\cdot)$ and the limit point is shown by (o) on the figures.

the initial portion of the gelation. The zero of the second derivative, i.e. the inflection point of the gelation curve is shown by $(*)$, while the zero of the third derivative is denoted by $(+)$. The sequence of the absolute maxima of the even order derivatives are shown by $(.)$'s and the limit point is shown by (o) on these graphs. From these figures, it can be seen that the location of the gel point moves left, relatively closer to the zero of the third derivative as the parameter k increases.

5. Conclusion

5.1. *Discussion of the results*

In this paper, we proposed a new computational method for locating the critical point of a phase transition and applied it to the sol−gel transition of AAm with SA. We have already shown in Ref. 1 that the sol−gel transition above obeying the percolation law is represented by the SIR model. We have used the exact solution of the SIR model as a dynamical system to predict the position of the gel point as on the sigmoidal curves obtained in real experiments.

In this set-up, we considered the mathematical model for the gelation curve, represented by the function $R(t)$ of the SIR model and we computed the derivatives d^nR/dt^n for $n = 1, \ldots, 24$. We have plotted these derivatives as a function of t and we have observed that the time instants where the derivatives of even order reach their absolute extreme value, have a limit that we have denoted by t_c. Denoting the zeros of the third and the second derivatives of $R(t)$ as t_a and t_m, we have seen that the limit point t_c lies in between these points; i.e. $t_a < t_c < t_m$ and the exact location of t_c in the interval $[t_a, t_m]$ depends on the SIR model parameter k/η. We have seen that for higher values of k/η, the gel point t_c is relatively closer to t_a, while for lower values of k/η, t_c is closer to t_m.

The SIR models with higher values of k/η have sharper transition curves and they correspond to gelation curves where the polymerization and/or monomer consumption is faster. In the present paper, higher values of k/η correspond to lower SA concentrations. In the case of the SIR model the mathematically defined critical points found from the simulations agree qualitatively with the experimental results obeying the percolation type phase transitions presented in Fig. 2.

5.2. *Directions for future work*

In preliminary work leading to the present paper, we have computed higher derivatives and studied the location of the critical point for a number of mathematical functions representing symmetrical sigmoidal curves. We have observed that, they have more or less the same behavior in the sense that the critical point is always located at the inflection point. Here, we have presented the results for the logistic growth curve as a typical case (Fig. 1). To give an idea on the technical limitations, we note that we were able to compute the zeros of the derivatives of the logistic growth curve up to orders 200 but we could plot only the first 30 derivatives. The

location of the critical point for nonsymmetrical sigmoidal curves represented by the generalized logistic equation is currently studied; preliminary results has shown that, as in the case of the SIR model, the critical point moves earlier in time as the asymmetry of the sigmoidal curve increases.

We recall that the availability of the exact solution of the SIR model was crucial in being able to compute higher derivatives. We were able to obtain analytical expressions for the higher derivatives up to orders 30−40 easily with the symbolic programming REDUCE, then we were able to plot these simultaneously up to orders 30. On the other hand, for the SEIR model that represents the gelation of the same system obeying the classical law, we had to use numerical solution curves. With the present state of our computational tools, derivatives up to orders 10−20 were numerically stable and we could not locate the critical point. We are currently working on more sophisticated numerical schemes to increase the accuracy of the solutions.

We note that all of the gelation experiments described in Sec. 2.2 need not obey the SIR or the SEIR models. Among the experiments described therein, the gelation of AAm monitored with SSF technique (e) obeys the SIR and SEIR models respectively for the percolation type and classical gelation. We expect that sigmoidal curves given by the experiments with SSF will also obey the same models.

The classical gelation models whose exact solution is given by the Flory−Stockmayer theory predicts the gel point to occur at the probability $p_c = 1/(z-1)$ where z is the functionality of the molecules. It is thus of prime importance to be able to locate the critical point for the SEIR model, which has been found to be adequate at least for the gelation of the AAm.

The gelation experiments described in (a) and (b) obeys percolation theory but the location of the critical point as given in Ref. 9 is closer to the zero of the second derivative, hence there is need for further investigation for modeling these gelation mechanisms.

The reversible gelation experiments described in (f), provide full sigmoidal curves as functions of temperature, despite the fact the pre-critical-point exponents are not determined. As part of ongoing work we note that, these curves do not obey the SIR or the SEIR models, but they follow the steady state value of R_f of $R(t)$ as a function of the parameter k/η in the SIR model.

The experiments (c), (g) and (h) which are only the post-critical-point part of the sigmoidal curve was recorded, hence mathematical models for these gelation processes will not be studied in near future.

Acknowledgments

This work is partially supported by The Scientific and Technological Research Council of Turkey (TUBITAK).

References

1. A. H. Bilge, O. Pekcan and V. Gurol, *Application of Epidemic Models to Phase Transitions*, Phase transitions, **85**, 1009 (2012).
2. G. A. Evingur, F. Tezcan, F. B. Erim and O. Pekcan, *Phase Transit.* **85**, 530 (2012).
3. P. J. Flory, *J. Am. Chem. Soc.* **63**, 3083 (1941).
4. W. H. Stockmayer, *J. Chem. Phys.* **11**, 45 (1943).
5. D. Stauffer, A. Coniglio and M. Adam, *Adv. Polym. Sci.* **44**, 103 (1982).
6. D. Stauffer, *Introduction to Percolation Theory* (Taylor and Francis, London, 1985).
7. H. Herrmann, *Phys. Rep.* **136**, 153 (1986).
8. D. Stauffer and A. Aharony, *Introduction to Percolation Theory* (Taylor and Francis, London, 1992).
9. Y. Yilmaz, A. Erzan and O. Pekcan, *Phys. Rev. E* **58**, 7487 (1998).
10. O. Pekcan and D. Kaya, *Compos. Interfaces* **12**, 501 (2005).
11. Z. Dogruyol, N. Arsu and O. Pekcan, *J. Macromol. Sci. B Phys.* **48**, 745 (2009).
12. D. Kaya, O. Pekcan and Y. Yilmaz, *Phys. Rev. E* **69**, Article Number 016117 (2004).
13. H. Ozbek and O. Pekcan, *J. Mol. Struct.-Theochem.* **676**, 19 (2004).
14. O. Tari, S. Kara and O. Pekcan, *J. Macromol. Sci. B Phys.* **48**, 812 (2009).
15. O. Tari, S. Kara and O. Pekcan, *J. Appl. Polym. Sci.* **121**, 2652 (2011).
16. D. K. Aktas, G. A. Evingur and O. Pekcan, *J. Biomol. Struct. Dyn.* **24**, 83 (2006).
17. D. K. Aktas, G. A. Evingur and O. Pekcan, *Compos. Interfaces* **17**, 301 (2010).
18. G. Polya, *Bull. Amer. Math. Soc.* **49**, 178 (1942).
19. H. W. Hethcote, *SIAM Rev.* **42**, 599 (2000).
20. W. O. Kermack and A. G. McKendrick, *Proc. R. Soc.* **115A**, 700 (1927), Reprinted in *Bull. Math. Biol.* **53**, 33 (1991).
21. D. R. Souza, T. Tome and R. M. Ziff, *J. Stat. Mech.: Theory Exp.*, p03006 (2011).
22. M. Gordon, *Proc. R. Soc. Lond. A* **268**, 240 (1962).
23. C. W. Macosko and D. R. Miller, *Macromolecules* **9**, 199 (1976).
24. D. S. Pearson and W. W. Graessley, *Macromolecules* **11**, 528 (1978).
25. D. Durand and C. M. Bruneau, *J. Polym. Sci. B Polym. Phys.* **17**, 273 (1979).
26. S. Hellerstein and J. Williamson, *Bull. Amer. Math. Soc.* **81**, 453 (1975).
27. W. Bergweiler and A. Eremenko, *Acta Math.* **197**, 145 (2006).